Control of the Morphogenesis of Barium Chromate by Using Double-Hydrophilic Block Copolymers (DHBCs) as Crystal Growth Modifiers

Shu-Hong Yu,* Helmut Cölfen,* and Markus Antonietti[a]

Abstract: A systematic morphosynthesis of barium chromate particles has been performed by using double-hydrophilic block copolymers (DHBCs), which consist of a hydrophilic solvating block and a hydrophilic binding block, as crystal growth modifiers to direct the controlled precipitation of barium chromate from aqueous solution. Several kinds of DHBCs with different functional groups $-COOH$, $-PO_3H_2$, $-SO_3H$, $-SH$ as well as PEG-poly(aminoamine) block-dendrimer copolymers were explored for crystallization and morphology control of barium chromate. Well-defined morphologies of $BaCrO_4$ particles can be produced, such as more or less dendritic X-shaped, elongated X-shaped, or rodlike particles, flower-like plates, ellipsoids, spheres, nanofiber bundles, nanofibers, and other more complex morphologies. In the presence of the phosphonated copolymer PEG-*b*-PMAA-PO_3H_2 (degree of phosphonation: 21%) at pH 5, large conelike bundles of nanofibers ranging from 10 to 20 nm in diameter with lengths up to 150 μm can be produced at room temperature, whereas replacement of the covalently bound phosphonate groups by the ionic salt analogue dopant fails to produce this structure, indicating the importance of the functional polymer block structures. The time-resolved formation process of the bundles of nanofibres was investigated, showing a remarkable self-similarity. At temperatures higher than 50 °C, in plastic flasks or when undergoing continuous stirring, only ellipsoids or nearly spherical particles can be obtained. This shows that the fiber formation relies on heterogeneous nucleation and is in agreement with a recently published mechanism where fiber formation is due to the vectorially directed self-assembly of primary particles. Our results demonstrate that the integration of DHBCs, taking advantage of the experimental conditions such as crystallization sites, temperature, pH, and reactant concentration, will extend the possibilities for controlling the shape, size, and microstructures of the inorganic crystals by means of a simple mineralization process.

Keywords: barium chromate · block copolymers · colloids · morphogenesis · self-organization · superstructures

Introduction

Synthesis of inorganic crystals with specific size and morphology has recently attracted a lot of interest because of the potential to design new materials and devices in various fields such as catalysis, medicine, electronics, ceramics, pigments, and cosmetics.[1–4] Shape control and exploration of novel methods for self-assembling or surface-assembling molecules or colloids to generate materials with controlled morphologies and unique properties have been undertaken in recent years. For example, shape control has significant relevance in the fabrication of semiconductor nanocrystals,[3] metal nanocrystals,[4] and other inorganic materials,[1, 2] which may add additional variables in tailoring the properties of nanomaterials. Much effort has been made in the fabrication of one-dimensional nanowires or nanorods[5–8] by using hard templates such as carbon nanotubes[5, 6] and porous aluminum templates,[7] or by laser-assisted catalytic growth (LCG),[8] as well as controlled solution growth at room or elevated temperature.[3, 9]

In addition, bioinspired morphosynthesis strategies have also been explored to template inorganic materials with controlled morphologies by using self-assembled organic superstructures, organic additives, and/or templates with complex functionalization patterns.[1, 10] The precipitation of inorganic molecules with three-dimensional lipid and protein structures has been found to generate unusual morphologies such as oblong crystallites, mineralized organic tubules and disks, and microporous reticulated structures.[11, 12] Reverse micelles and microemulsion techniques have been widely used for the preparation of copper nanorods,[4c] higher-order structures such as $BaCrO_4$ chains and filaments,[1d] $BaSO_4$

[a] Dr. S.-H. Yu, Dr. H. Cölfen, Prof. Dr. M. Antonietti
Max Planck Institute of Colloids and Interfaces
Department of Colloid Chemistry
MPI Research Campus Golm, 14424, Potsdam (Germany)
Fax: (+49) 567-9502
E-mail: shyu@mpikg-golm.mpg.de, coelfen@mpikg-golm.mpg.de

Supporting information for this article is available on the WWW under http://wiley-vch.de/home/chemistry/ or from the author.

  0947-6539/02/0813-2937 $ 20.00+.50/0

filaments and cones,[13] as well as $CaSO_4$[14] and $BaCO_3$ nanowires[15] at room temperature.

Currently, hashemite, the naturally occurring chromate analogue of barite, together with barite has been widely used as a model system for morphosynthesis and kinetic crystallization studies as they crystallize only in a single modification. Hashemite can also be used as an oxidizing agent and catalyst to carry out vapor-phase oxidation reactions.[16] Most previous reports focus on barite. In contrast, hashemite has rarely been studied. Prior to this report, an extra-slow precipitation technique of X-shaped and hexagonal plates and other, more complicated, forms of barium chromate particles was reported as early as 1961.[17] Later, Mann et al. described the synthesis of ordered microarrays of nanocrystals of both barium chromate and sulfate,[1d] which demonstrated the possibility of controlling both the morphology and the mutual orientation, and micelles as well as microemulsions have been used as templates for the synthesis of barite nanofilaments.[13] On the other hand, several kinds of organic additives have been used as crystal modifiers to direct the nucleation and growth of barite from aqueous solution.[18, 19] Whiting et al. reported the design of a family of macrocyclic aminomethylphosphonates for the purpose of recognizing, and binding to all of the important growing faces of barite, and thus promoting isotropic growth.[20] Previous work has shown that the phosphonate group is a good match for sulfate sites in the barium sulfate lattice.[21, 22]

Although various examples of shape control have been demonstrated, exploration of the facile synthesis of inorganic crystals with controllable size and shape in aqueous solution at room temperature remains nonsystematic and challenging. Recently, it was shown that double-hydrophilic block copolymers (DHBCs)[23] can exert a strong influence on the external morphology and/or crystalline structure of inorganic particles such as calcium carbonate,[24] calcium phosphate,[25] barium sulfate,[26] and zinc oxide.[27]

Herein, we demonstrate a rather flexible morphosynthesis of hashemite by using DHBCs as crystal modifiers. The morphology can be systematically controlled by variation in functional group and molecular structure of the DHBC copolymers. Other effects such as the crystallization sites, temperature, pH, reactant concentration, and copolymer concentration on the morphology were also examined. The results demonstrate that the integration of DHBCs, taking advantage of other experimental conditions, will provide more possibilities for the controlled synthesis of inorganic crystals with well-defined shape, size, and microstructures.

Results and Discussion

Control of the morphogenesis of $BaCrO_4$: In the absence of polymeric additives, the precipitation process of $BaCrO_4$ occurs very quickly, and the solution always became turbid in less than 6 min. All of the obtained products were revealed to be well-crystallized hashemite crystals according to the corresponding XRD results (see Figure 1 in the Supporting Information). All diffraction peaks can be indexed with reference to the unit cell of the hashemite structure (JCPDS Card: 15-376, $a = 9.105$, $b = 5.541$, $c = 7.343$ Å, space group *Pnma* [D_h^{16}]). Figure 1a shows that the crystals obtained in the absence of additives exhibit dendritic X-shaped crystals with an average length of about 10 μm. The observed more-or-less dendritic X-shaped morphology is similar to that obtained by an extra-slow precipitation technique reported as early as 1961.[17] It has been reported that there are eight faces important for the crystal growth of barite—(210), (001), (211), (100), (101), (011), (010), and (111)[28a–b]—which will be also

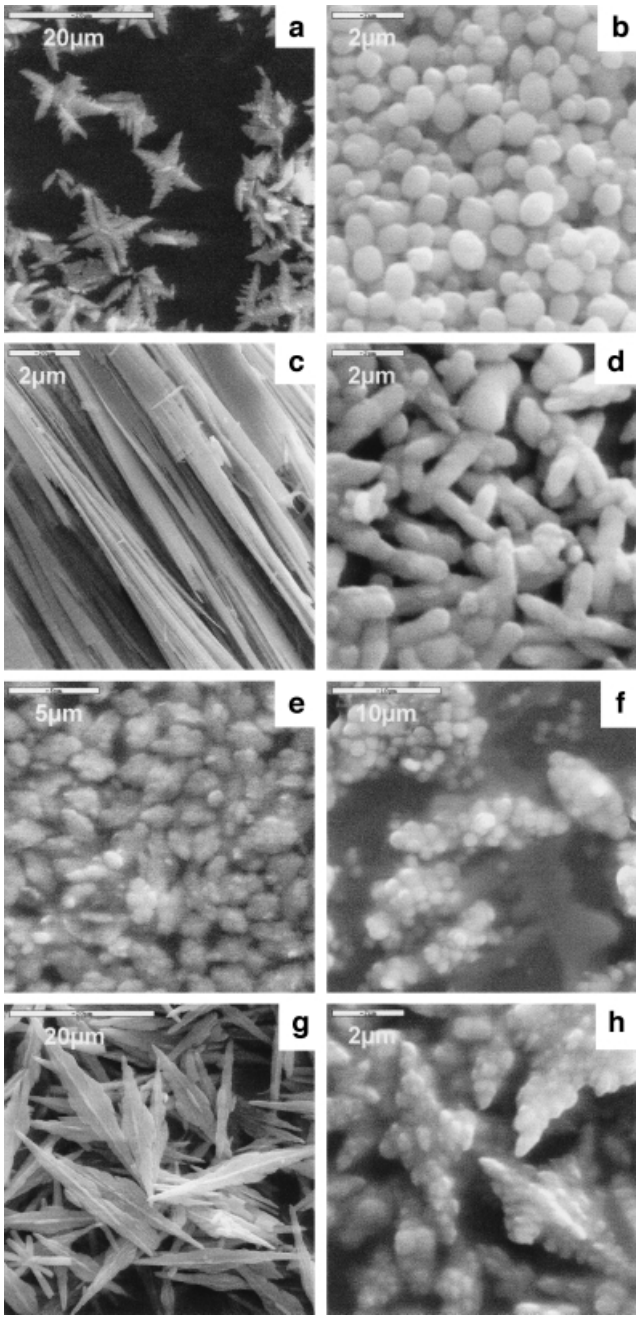

Figure 1. Typical SEM images of the manipulation of $BaCrO_4$ morphologies by DHBCs, the polymer concentration was kept at $1\,g\,L^{-1}$ ($[BaCrO_4] = 2$ mM), pH 5: a) no additive; b) PEG-*b*-PMAA; c) PEG-*b*-PMAA-PO_3H_2 (degree of phosphonation: 21%); d) PEG-*b*-PEI-$(CH_2{-}CH_2{-}PO_3H_2)_n$; e) PEG-*b*-PHEE-$PO_4H_2$ (degree of phosphonation: 30%); f) PEG-*b*-PEI($CH_2{-}CH_2{-}PO_3H_2$)-$COC_{11}H_{23}$; g) PEG-*b*-PEI$(CSHN{-}CH_3)_n$-$C_{11}H_{23}$; h) PEG-*b*-PEI-$(CH_2{-}CH_2{-}CH_2{-}SO_3H_2)_n$.

  0947-6539/02/0813-2938 $ 20.00+.50/0 *Chem. Eur. J.* **2002**, *8*, No. 13

applicable for hashemite since they have a similar structure and can form a solid solution.[28c] The relative diffraction intensity of either (200)/(002) or (210)/(002) is unusually higher than that reported (JCPDS Card: 15-376), and furthermore, only six out of the eight important faces are found, indicating the preferential orientation growth of the particles.

In contrast, the XRD patterns obtained in the presence of poly(ethylene glycol)-*block*-poly(ethylene imine)-poly(acetic acid)(PEG-*b*-PEIPA)[23b,c] and phosphonated poly(ethylene glycol)-*block*-poly(methacrylic acid) (PEG-*b*-PMAA-PO_3H_2)[24a] show significant differences to that obtained in the absence of an additive. The diffraction peaks become broader, indicating that the crystals are significantly smaller than those in the absence of polymer and, again, can be indexed as the hashemite structure (JCPDS Card: 15-376). In the case of using PEG-*b*-PMAA-PO_3H_2, a similar XRD pattern was obtained.

The particles obtained in the presence of PEG-*b*-PEIPA were found to be egg-shaped with an overall size of 100–180 nm. Egg-shaped particles with a size of 1 μm were also obtained with PEG-*b*-PMAA as a modifier, as shown in Figure 1b. The inhibition effect of PEG-*b*-PMAA for hashemite crystallization was found to be comparable to that of PEG-*b*-PEIPA, which coincides with the results reported for barite crystallization.[26c]

For the phosphonated derivative PEG-*b*-PMAA-PO_3H_2 (degree of phosphonation: 21%), nanofiber bundles were obtained (Figure 1c). On the other hand, rodlike particles with dimensions of 0.6×2 μm were produced in the presence of the phosphonated poly(ethylene glycol)-*block*-poly(ethylene imine) (PEG-*b*-PEIPEPA(PEG-*b*-PEI-(CH_2–CH_2–PO_3H_2)$_n$)[23c] (Figure 1d). When another phosphorus containing copolymer, the partially phosphorylated poly(hydroxy ethyl ethylene) block copolymer (PEG-*b*-PHEE-OPO_3H_2 (degree of phosphonation: 30%))[29] was used, the morphology changed to smaller, trapezoidal aggregates with no clear expression of faces (Figure 1e). It is delineated that this polymer is not purely hydrophilic anymore, but shows amphiphilic character and surface activity.[29]

As expected, a more pronounced partial hydrophobic modification of the functional polymer block results in mutual aggregation of the DHBCs and therefore an altered modification pattern, resulting also in altered mineralized superstructures. When the PEI backbone of PEG-*b*-PEI-(CH_2–CH_2–PO_3H_2) was additionally modified with lauroyl-$COC_{11}H_{23}$ moieties (PEG-*b*-PEI(CH_2CH_2–PO_3H_2)-$COC_{11}H_{23}$),[23c] the hybrid superstructures are composed of smaller aggregated spheres clustered together as shown in Figure 1f, and the rodlike structure obtained with the non-hydrophobically modified polymer (Figure 1d) is lost. Uniform, well-defined lancet-like particles with a length of 20 μm and a width of 5 μm were obtained in the presence of PEG-PEI($CSHNCH_3$)$_n$-$COC_{11}H_{23}$ (Figure 1g). Apparently, in this case, the hydrophobic modification does not lead to clustered, aggregated spheres as found for the phosphonated polymer analogue, suggesting a site-selective block copolymer adsorption. The aspect ratio of *a*/*b* is as large as 5–5.4 (Figure 1g), which is much higher than that previously observed in the case of barite,[18] an observation that supports site-selective block copolymer adsorption.

If sulfonated poly(ethylene glycol)-*block*-poly(ethylene imine) (PEG-*b*-PEI-(CH_2–CH_2–CH_2–SO_3H_2)$_n$) was used (a poly-zwitterionic amphiphile), more elongated clusters of compact particles were obtained, where the shape of the cluster adopts the morphology of the lancets (Figure 1h), suggesting an overgrowth of previously formed lancets.

All DHBCs based on a bare PEI binding site have comparatively little control over the oriented growth of the crystals under the applied acidic conditions at pH 5, underlining the fact that the growing crystals prefer to interact with the negatively charged $-PO_3H_2$ and $-COOH$ groups instead of the positively charged PEI block. Only PEG-STARBURST, which containes a rigid dendrimer (with a broad distribution of pK_a values) as the modifying functional unit, shows a weak inhibition, and the morphology was found to possess three-dimensionally, rectangular branched characteristics (data not shown).

Complexity, similarity of fiber bundles and possible formation mechanism: More complex morphologies of hashemite can be formed in the presence of PEG-*b*-PMAA-PO_3H_2. Figure 2a and 2b show SEM images of thin, flexible planes with sharp edges composed of densely packed, highly ordered, parallel nanofibers of $BaCrO_4$. Figure 3b shows two fiber bundles with a fanlike shape and length about 15 μm. Here, it may be

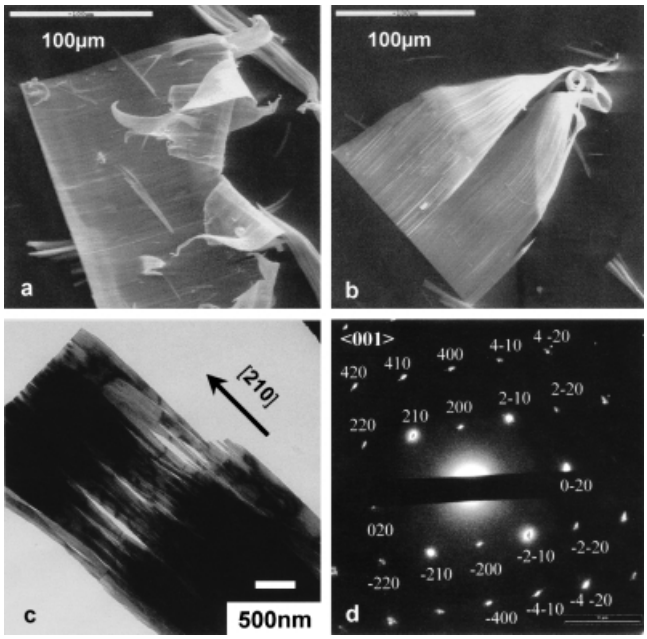

Figure 2. SEM and TEM images of highly ordered $BaCrO_4$ nanofiber bundles obtained in the presence of PEG-*b*-PMAA-PO_3H_2 (degree of phosphonation: 21%) (1 g L^{-1}) ([$BaCrO_4$] = 2 mM), pH 5: a) SEM image shows the very thin fiber bundles; b) two fiber bundles with conelike shape and length about 150 μm; c) TEM image of the thin part of the fiber bundles; d) electronic diffraction pattern taken along [001], showing that the fiber bundles are well crystallized single crystals and elongated along [210].

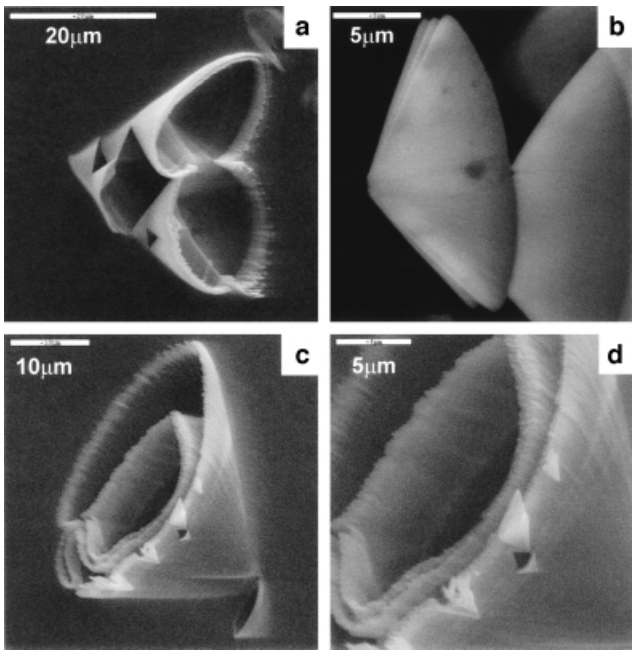

Figure 3. Typical $BaCrO_4$ multi-funnel-like superstructures with remarkable self-similarity in the presence of PEG-*b*-PMAA-PO_3H_2 (degree of phosphonation: 1%) (1 gL^{-1}) ([$BaCrO_4$] = 2 mM, pH 5), showing that the superstructures are composed of several very thin layer fiber bundles with flat "funnel" edges.

seen that each of those superstructures nucleate from single heterogeneous sites, but grow and fuse towards highly parallel planes, as detected by their common sharp growth plane. The TEM image with higher resolution in Figure 2c clearly shows the self-organized nature of the superstructure. Whereas the majority of the fibers appear to be aligned in a parallel fashion, gaps between the single fibers can form, but are also closed again. An electronic diffraction pattern taken from such an oriented planar bundle as shown in Figure 2d confirmed that the whole structure scatters as a well crystallized single crystal where scattering is along the [001] direction and the fibers are elongated along [210].

The atomic surface structure modeling data for the surface cleavage of the hashemite crystal (see Figure 2 in the Supporting Information) shows that the faces (1 – 22), (1 – 21), (1 – 20), (– 120), which are parallel to the [210] axis, contain slightly elevated barium ions, indicating that the negatively charged $-PO_3H_2$, and –COOH groups of PEG-*b*-PMAA-PO_3H_2 can preferentially adsorb on these faces by electrostatic attraction and block these faces from further growth. In contrast, surface cleavage of the (210) face shows no barium ions on the surface that are susceptible to attack, suggesting that the functional polymer group does not favorably adsorb on this face leading to a fast growth rate. This is favorable for orientation growth along the [210] direction. Surface cleavage of the (2 – 10), and (– 210) faces shows that these surfaces are neutral, that is, are composed of strictly alternating Ba^{2+} and CrO_4^{2-} ions. Both polymer adsorption and crystal growth are expected to be weak along these faces, and indeed, the primary crystals lie in a vectorial fashion along these faces, coexisting as the ribbon structures shown in Figure 2c.

The fact that the structure is composed of single fibers, but scatters as a single crystal in two dimensions, underlines the perfect vectorial orientation of the building blocks, that is there is no translational or rotational disorder between each crystal unit cell of the system, and—although not connected—they are locked in a periodic force field. This is in addition to our previous findings where we discussed a vectorial direction of crystalline bricklike building units which fuse together to build up $BaSO_4$ nanofibers.[26c] Here, we observe that the fibers are grown along a single orientation direction and self-organize into a two- or three-dimensional superstructure, suggesting that in addition to the vectorially directed fiber formation, forces also act perpendicular to the fiber axis, which control their interspacing. However, as discussed above, gaps may occur and furthermore, the fiber bundles originate from a single point due to their heterogeneous nucleation so that the finding of fibers that are perfectly aligned in two dimensions only holds for the later development (see Figure 2b).

Evidently, in accord with our earlier findings for barite crystallization, a block copolymer with a combination of carboxyl and phosphonate groups has a strong morphology-directing influence towards fiber formation, although the degree of phosphonation was rather low (21%).[26c] To test if even spurious degrees of phosphonation, in conjunction with carboxyl groups, can exert a directing influence, we prepared a PEG-*b*-PMAA with very little phosphonation (ca. 1%, but experimentally hard to quantify). In contrast to the egg-shaped superstructures as found for the pure PEG-*b*-PMAA (see Figure 1b), we obtained fused cones composed of nanofibers and also a multi-cone-like superstructure that shows a remarkable self similarity (see Figure 3). This demonstrated that a small proportion of phosphonate groups is able to dominate over a majority of carboxyl functionalities. A control experiment where the crystallization was carried out in the presence of 1 gL^{-1} PEG-*b*-PMAA and an appropriate amount of Na_2HPO_3 as the functional low molecular weight analogue, only yielded egg-shaped particles as for pure PEG-*b*-PMAA. Thus, it is confirmed that a small amount of phosphonate groups covalently bound to a PMAA block is sufficient for the formation of fiber bundles.

The ability of the edges to attract each other and fuse leads to the simultaneous occurrence of thin, very filigree fused cones (see Figure 3a and 3b). The conelike superstructures tend to grow further into a self-similar, multi-cone "tree" structure which was observed before for barite mineralized in the presence of polyacrylates, but only under very limited experimental conditions.[26c] While closely inspecting the detailed structures of the conelike bundles, many of them were found to be in the form of cone-in-a-cone "matrioshka" structure, as clearly shown in the zoom series of Figure 3c and 3d.

This superstructure developed more clearly, and to much larger sizes, when the mineralization temperature was lowered to 4 °C as shown in Figure 4a and 4b. The bigger size is due to a lowered nucleation rate. Due to their size and the related weight, the cones collapse, at least in the dried state depicted by SEM. From the higher magnifications of the same structures shown in Figure 4c and 4d, a number of facts become obvious.

  0947-6539/02/0813-2940 $ 20.00+.50/0 *Chem. Eur. J.* **2002**, *8*, No. 13

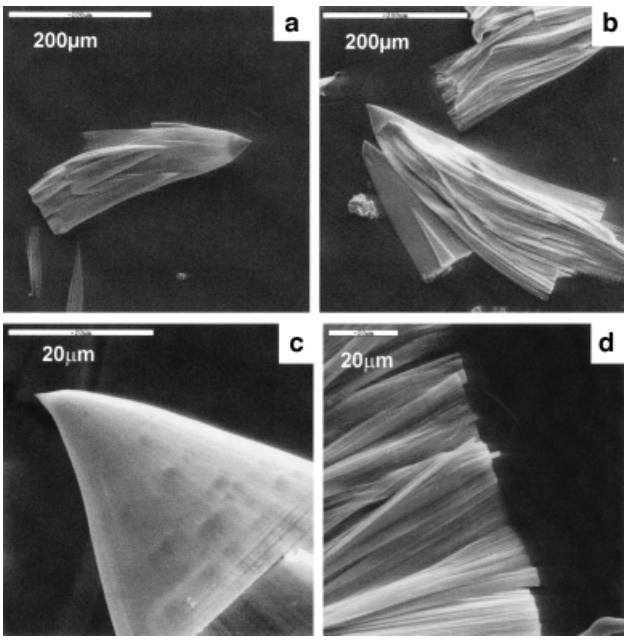

Figure 4. Typical conelike superstructure containing densely-packed $BaCrO_4$ nanofiber bundles in the presence of PEG-*b*-PMAA-PO_3H_2 (degree of phosphonation: 21%) (1 g L^{-1}) ([$BaCrO_4$] = 2 mM, pH 5): a, b) 4 °C; c) the "tip" of the cone; d) the "end" of the cone.

- All structures always grow from a single starting point. This may be the glass wall or other substrates such as TEM grids, which provide the necessary heterogeneous nucleation sites.
- The growth front is always very smooth (Figure 4c), suggesting that the homogeneous joint growth of all single nanofilaments even has the ability to cure occurring defects. This is in line with our earlier findings for $BaSO_4$.[26c]
- The opening angle of the cones is always rather similar when considering a constant ratio of longitudinal to transverse growth. The opening angle seems to depend on temperature, degree of phosphonation of the polymer, and polymer concentration. The control experiments show that the higher the temperature, the more linear the structures become (see Figure 3a and 3b in the Supporting Information).
- Secondary cones can nucleate from either the rim or defects on the cone, thus resulting in treelike structures.
- The fact that a cone stops growing once a second cone has nucleated at one spot on the rim shows that growth is presumably slowing down with time, favoring the growth of the secondary cone. This was recently discussed by a variety of authors as a consequence of the influence of electrostatic-dipole and multipole fields of the superstructure on approaching ions and colloidal building blocks, resulting in branching instead of further growth.[26c, 30] A similar effect is that ripened cones (such as the matrioshkas shown in Figure 3c and 3d) show a frayed overgrowth of the rim by secondary crystals, underlining that the primary crystallization mechanism has become ineffective.
- Due to drying, the cones can disintegrate towards single-fiber bundles, showing that the cohesion between the single fibers is weak, that is these are secondary interactions and not crystalline forces aligning the fibers.

To shed some light on the nucleation process of the fiber bundles, time-dependent transmission electron microscopy experiments were conducted. Figure 5 shows representative pictures of the early growth stage of the fiber bundles. Figure 5a depicts the early stages of precipitation (after 4 h).

As already described for calcium carbonate[24b, 29] and barium sulfate,[26c] the initially formed particles are amorphous with sizes of up to 20 nm, which can aggregate to larger clusters. Evidently, this state of matter is the typical starting point for all types of highly inhibited reactions. The very low ion product of barium chromate ($K_{sp} = 1.17 \times 10^{-10}$) shows that the superstructures do not really grow from a supersaturated ion solution but by aggregation/transformation of the primary clusters formed. This is in perfect agreement with earlier findings that in an ion solution with concentrations far above the saturation level, amorphous clusters are formed first, which then produce the crystalline nuclei at a later stage.[31] After one day, the first conical fiber bundles were found on the TEM grids as shown in Figure 5b. Indeed it is seen that they start their life from a single nucleation site and grow/multiply from the beginning in the same way seen on larger scales by SEM. One can also distinguish some isolated amorphous nanoparticles supporting the growth of the fibers. Figure 5c shows another typical case with a start point and developing and growing fiber bundles, and a lot of amorphous particles at the end (growing point) (see inserted ED pattern in Figure 5c).

A complete mechanism of the development of the multicone-like superstructures is proposed. This is shown in Scheme 1: i) At the beginning, amorphous particles are formed which are stabilized by the DHBCs (stage 1); ii)

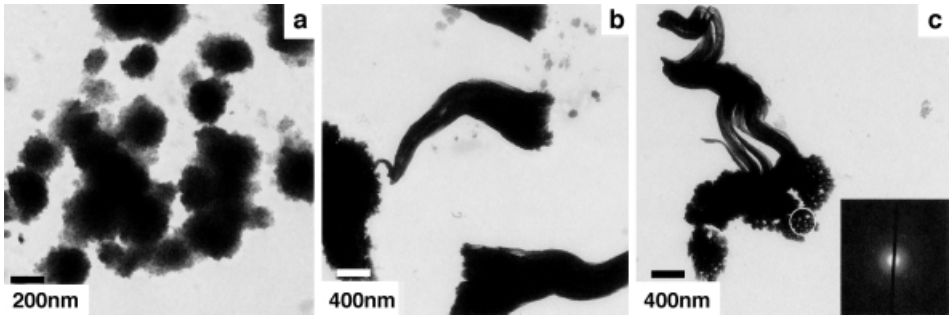

Figure 5. TEM images showing the evolution process of growth of the fiber bundles that formed on TEM grids in the presence of PEG-*b*-PMAA-PO_3H_2 (degree of phosphonation: 21%), 1 g L^{-1}, [$BaCrO_4$] = 2 mM, in a polypropylene (PP) tube after reaction for a) 4 h; b) 24 h; c) TEM images and inserted electronic diffraction patterns showing the evidence of growth of the fiber bundles from the aggregation and connection of the amorphous particles that formed on TEM grids in a polypropylene tube after reaction for 4 days: a typical fiber bundle showing that it grew from a start point and with a lot of amorphous particles on the end. PEG-*b*-PMAA-PO_3H_2 (degree of phosphonation: 21%), 1 g L^{-1}, [$BaCrO_4$] = 1 mM.

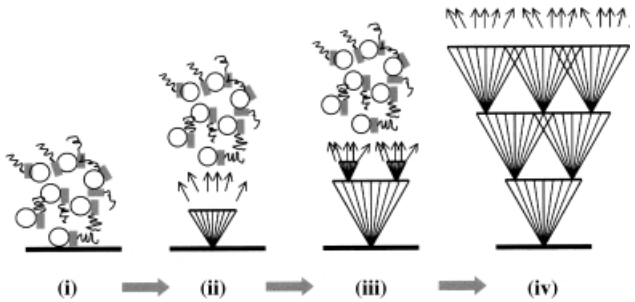

Scheme 1. Proposed mechanism for the formation of complexity superstructure with self-similarity.

heterogeneous nucleation of fibers occurs on glass substrates and the fibers grow under control of DHBCs, presumably by multipole field-directed aggregation of amorphous nanoparticles (stage 2, for a closer view on multipole field directed crystallization, see ref. [30d]); iii) the growth is continuously slowed down until secondary nucleation or overgrowth becomes more probable than the continuation of the primary growth. This is a statistical observation and will lead to a distribution of cone sizes. The secondary cone will grow as the first ones have done; iv) the secondary heterogeneous nucleation taking place on the rim can occur repeatedly depending on the mass capacity of amorphous nanoparticles in the system.

A plausible reason for the self-limiting growth may be seen in the crystal structure of hashemite/barite. These crystals have a mirror plane perpendicular to the *c* axis, which means that a homogeneous nucleation will always result in crystals with identical charges on the opposite faces. Thus, no dipole crystals can be formed. For heterogeneous nucleation, the situation is different. A dipole crystal may be favored as one end of the crystal is determined by the heterogeneous surface, the other by the solution/dispersion. Accordingly, it has a dipole moment $\mu = Q \cdot l$ (Q = charge and l = length of the crystal) which increases while the crystal is growing. This implies self-limiting growth so that a new heterogeneous nucleation on the rim should become favorable after the dipole moment has reached a critical value due to energy minimization. Such a self-limiting growth mechanism would also explain why the growth edge is so uniform.

The whole suggested mechanism relies on the absence of flow, which would disturb the directed diffusion and aggregation according to local dipole/multipole fields. No fiber bundles or cones were obtained if the solution was stirred continuously at room temperature after mixing the reactants. Instead, only irregular and nearly spherical particles were obtained. This is again in agreement with a recently published mechanism where the fiber formation is due to the directed self-assembly of the primary particles,[26c] which is suppressed by stirring.

Effects of molar ratios, the concentration of reactants, and pH on the morphology in the presence of PEG-*b*-PMAA-PO_3H_2 (21% phosphonated): In the case of the polymer that has the strongest interaction with the mineral, we also performed a series of concentration studies to identify optimal concentration conditions. When the concentration of both ions was equimolar ($[Ba^{2+}]:[CrO_4^{2-}] = 1:1$) and was as low as 0.025 M (in the presence of 1 gL^{-1} of the copolymer), no precipitation occurred even after aging for three weeks at room temperature although the reference experiment without polymer showed crystallization. This shows that the polymers are able to stabilize the precursor particles at this concentration level without the ability to undergo further structural transitions. When the concentration was increased up to 0.05 M, structured crystallization occurred after one to four days. Further increase of the ion concentration up to 0.2 M resulted in very quick precipitation. TEM shows that in this case, only ellipsoids or boulder-like crystals with sizes of about 200–600 nm were produced (see Figure 4 in the Supporting Information).

If the $[Ba^{2+}]:[CrO_4^{2-}]$ molar ratio was changed to 1:5, the solution became turbid as soon as Na_2CrO_4 was added to the system. Again, no strong control was exerted by the polymer, and only ellipsoidal nanoparticles or aggregates with sizes ranging from 300 nm to 800 nm could be obtained. Similarly, when the $[Ba^{2+}]:[CrO_4^{2-}]$ molar ratio was changed to 2.5:1 (the polymer concentration was still kept as 1 gL^{-1}), unstructured nanoparticles with sizes of 60 to 100 nm were once more obtained (see Figure 4 in the Supporting Information).

These results show that the polymer essentially interacts with "neutral" crystals that show no overall surface enrichment of either one or the other ionic species. This mode of interaction is clearly different from the previous observation of a microemulsion system, in which the higher aspect ratios of $BaCrO_4$ nanofilaments were found only at a higher $[Ba^{2+}]:[CrO_4^{2-}]$ molar ratio (5:1),[1d] that is the interaction with the anionic AOT surfactants of this particular system is mediated by the excess of barium ions. Based on the molecular-modeling calculation results, the dimension of one chromate anion is about 3.3 Å, and the active functional dimensions of the groups $-PO_3H_2$, $-COOH$ are 3.5, and 2.2 Å, respectively. Therefore, a chromate ion can be favorably replaced by a phosophonate group but not by a carboxyl group, which may explain the extraordinary affinity of phosphonate groups for the hashemite crystal surfaces (see also refs. [21,22]). These results imply that the block copolymers do not only act by means of electrostatic attraction but also apparently replace negative chromate ions on the crystal surface. This finding is supported by the result that PEI blocks that show no match, but in principle can complex with surface sites, do not show any morphology directing influence.

When the concentration of the polymer was lowered to 0.2 gL^{-1}, the solution quickly becomes turbid, and the precipitate consistes of nanoparticles of almost spherical shape. This result suggests that the interaction capacity of the phosphonated copolymer at lower concentration is not high enough to stabilize the fibers with their high internal surface, but still shows strong interaction with all of the crystal faces. The result is nanoparticles instead of larger crystals. When the concentration of the polymer is increased up to 1 gL^{-1}, only fiber bundles are obtained as discussed before. Upon increase of the polymer concentration to 2 gL^{-1}, the solution stays transparent and yellow and a very loose flocculate is obtained after two or three days, which was found to be composed of aggregated, but not oriented, and therefore more dispersed fiber bundles (Figure 6).

  0947-6539/02/0813-2942 $ 20.00+.50/0 *Chem. Eur. J.* **2002**, *8*, No. 13

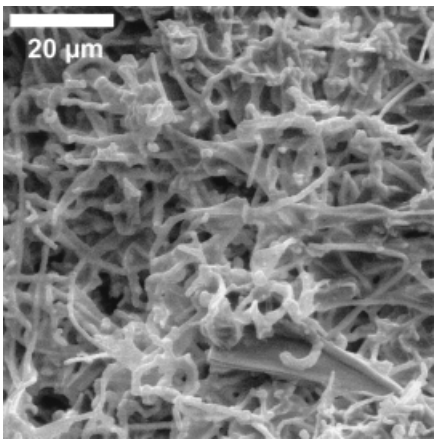

Figure 6. Effect of polymer concentration on morphology: PEG-*b*-PMAA-PO_3H_2 (degree of phosphonation: 21%), 2 gL^{-1}, [$BaCrO_4$] = 2 mM, glass bottle.

This ties in well with the idea of a strong interaction of the copolymer with the crystals, where the increased concentration leads to higher binding and a higher polymer content in the precipitate, making the hybrid morphology more dispersed. These results indicate that only a limited concentration window exists for the formation of three-dimensionally highly orientated fiber bundles. Apparently, the force responsible for the three-dimensional packing can be over-compensated by a high polymer surface coverage and the resulting steric and possible electrostatic repulsion.

When the pH was varied from 5.5 to 3.5, 2 respectively, no precipitate was found, even after aging for two weeks. The suitable pH range for the formation of $BaCrO_4$ fibers was within 5–7. In contrast, when the pH was changed to pH 10, the precipitate was found to be composed of nearly spherical particles in the µm range that formed a superstructure or aggregates of nanoparticles. This suggests that a selective adsorption of the block copolymer can only take place in a limited pH range whereas beyond the pH limits, the polymer adsorbs in a non-selective fashion.

Effect of the crystallization sites and temperature: The analysis of the growth of the fiber bundles suggests that the bundles grow from a single starting point where the glass wall, or other reaction vessel, provides the necessary heterogeneous nucleation sites. This is supported by a set of experiments where the reaction was conducted in polypropylene (PP) or plastic bottles. Here, only spherical particles can be obtained. If a carbon-coated copper TEM grid was put at the bottom of the plastic tube, long extended-fiber bundles grow from the TEM grid, but no fibers can be found on the plastic wall or bottom.

Increasing the temperature from 4 °C (conelike fiber bundles with large opening angle) over 25 °C (more linear and extended fiber bundles) to 50 °C results in faster nucleation and less specificity of the growth process. Small twinned or peanut-shaped nanoparticles were found at 50 °C (see Figure 5 in Supporting Information). Further increase of the temperature to 100 °C shows a continuation of this trend. Again, only peanut-shaped aggregates were found (Figure 7).

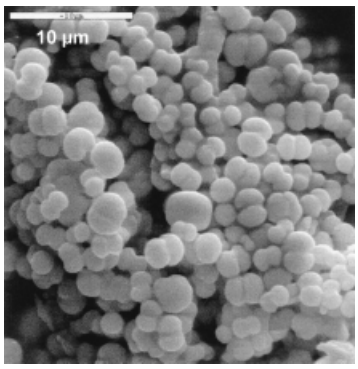

Figure 7. Effect of temperature on morphology: SEM image of peanut-like or twin structure of $BaCrO_4$ particles formed in the presence of PEG-*b*-PMAA-PO_3H_2 (degree of phosphonation: 21%), 1 gL^{-1}, [$BaCrO_4$] = 2 mM, glass bottle, 100 °C, 12 h.

This observation holds for both glass and polypropylene bottles, that is that higher temperatures indeed allow homogeneous nucleation to prevail over heterogeneous nucleation at lower temperatures, which leads to fibers. Here, a different species, the peanuts, where a nucleus can grow in two opposite directions, was found. Heterogeneous nucleation, presumably, has not stopped, but lost importance because of the acceleration of the homogeneous nucleation rate and the dominance of this stage of the crystallization process. Peanuts are formed at a much higher overall rate under this condition.

However, interestingly, not only nucleation must have changed, but also the growth mechanism, since in principle it should be also possible to grow fibers from continuous solution. Peanuts or dumbbells have already been found for a whole variety of species[24a,b,26a,b, 30] and are described as the product of a stopped-growth and crystal-branching process.[30b,d] It is therefore an open question whether twinning and the resulting coupled electrostatic multipole fields result in a maximized growth extension, whereas breaking the planar symmetry by addition of a surface or a heterogeneous nucleus can result in a continued build up of electrostatic fields and long extended fiber growth.

Conclusion

The present experiments demonstrate a systematic morphosynthesis of barium chromate crystals with controlled morphology and novel superstructures by using double-hydrophilic block copolymers (DHBCs) with varying patterns of functional groups. In addition, physicochemical parameters such as the crystallization sites, temperature, the concentration of reactants and the copolymers were examined and also showed significant effects on the morphology of the resulting particles, demonstrating that the ability of the copolymer to interact with the inorganic crystals could be fine-tuned. The main results are summarized in Scheme 2.

Using phosphonated polymers, it is possible to define conditions where fiberlike crystals with axial ratios larger than 10000 can be grown. The separation of these fibers depends on the amount of polymer and temperature, but they usually

  0947-6539/02/0813-2943 $ 20.00+.50/0

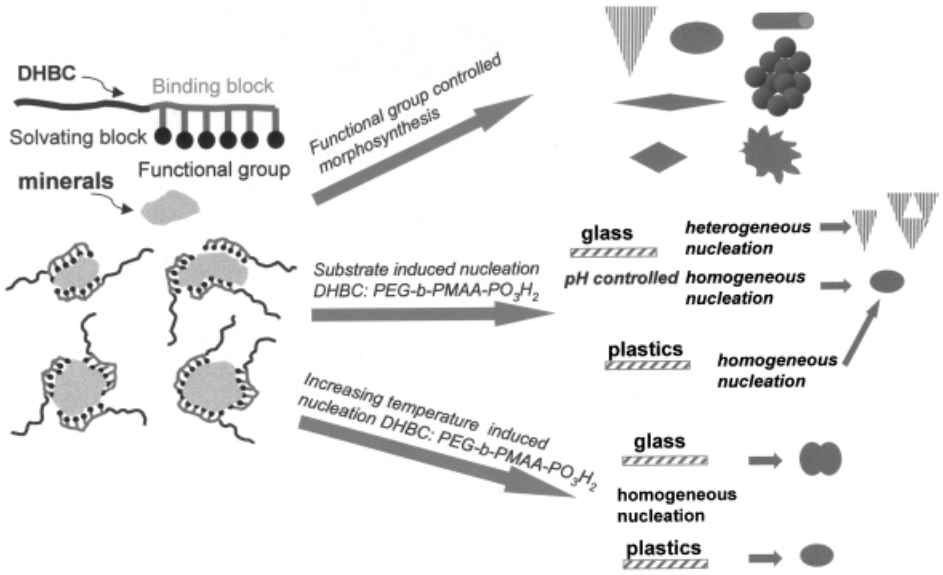

Scheme 2. Summary of the main results of a systematic morphosynthesis of hashemite by using double-hydrophilic block copolymers with different functional groups as crystal modifiers.

grow as sheets or bundles. The lower the temperature, the more extended and defined the fiber bundles become. It is remarkable that the fiber bundles and sheets show regions where the fiber bundles are perfectly aligned in two dimensions, including the fiber spacing, resulting in a single-crystal electron diffraction pattern. The sheets show self-alignment along their edges and can close to cones. Those cones can branch to form treelike structures, and a formation mechanism of the treelike superstructures is proposed. By variation of experimental conditions and using transmission electron microscopy, the heterogeneous nucleation of fibers, fiber bundles and cones was proven. We also confirmed a previous observation[26c] that the growth of such hybrid superstructures is promoted by the addition and recrystallization of primary colloidal particles rather than the build-up by single ions. It is also remarkable that spurious amounts of covalently linked phosphonate groups in conjunction with carboxyl groups in the PEG block copolymer direct the structure towards fibers, whereas doping of a PEG-*b*-PMAA solution with equal amounts of Na_2HPO_3 fails to produce such structures. This clearly indicates that the functional polymer block is responsible for the structure direction rather than a simple adsorption of single functional groups.

Using the same polymer and reactant concentrations but applying elevated temperatures, homogeneous nucleation becomes faster than heterogeneous nucleation, and peanut- or dumbbell-like particles are formed. Since it was impossible to grow fibers by homogeneous nucleation but only twinned structures with restricted size, it is speculated that the primary symmetry of the nuclei formed carries the character of an electrostatic multipole field, which is perpetuated and amplified throughout the growth process organized by the polymer. The detailed mechanism, however, needs further elucidation. Present experiments aim to control the heterogeneous nucleation by modification of the glassware (negative and positive charge) or by addition of highly polar colloidal nuclei. In addition, we want to follow the whereabouts and distribution of the polymer within the larger superstructures by confocal Raman microscopy and neutron scattering.

Our findings demonstrate that the combination of using DHBCs, taking advantage of other cooperative effects of experimental conditions such as the crystallization sites, temperature, pH, and reactant concentration, will extend the possibilities for the controlled synthesis of inorganic crystals with well-defined shape, size, and superstructures.

Experimental Section

Materials: All chemicals were obtained from Aldrich and used without further purification. Homopolymers poly(ethylene glycol) monomethyl ether (PEG, $M_W = 5000\,g\,mol^{-1}$) and poly(methacrylic acid, sodium salt) (PMAA, $M_W = 6500\,g\,mol^{-1}$) were purchased from Polysciences and Aldrich, respectively. A commercial block copolymer poly(ethylene glycol)-*block*-poly(methacrylic acid) (PEG-*b*-PMAA, PEG = 3000 g mol^{-1}, 68 monomer units, PMAA = 700 g mol^{-1}, 6 monomer units) was obtained from Th. Goldschmidt AG, Essen, Germany. The carboxylic acid groups of this copolymer were partially phosphonated (21 %) to give a copolymer with carboxyl and phosphonated groups, PEG-*b*-PMAA-PO_3H_2, according to ref. [24a]. The degree of phosphonation was determined with quantitative ^{31}P NMR spectroscopy by comparing the signals of an internal standard (KH_2PO_4 signal at $\delta = 3.1$ ppm) with the signal of the polymer product ($\delta = 18.6$ ppm) in D_2O.[32]

A block copolymer containing a poly(ethylenediaminetetraacetic acid) (EDTA)-like carboxy-functionalized block, poly(ethylene glycol)-*block*-poly(ethylene imine)-poly(acetic acid) (PEG-*b*-PEI-$(CH_2CO_2H)_n$, PEG-*b*-PEIPA, PEG = 5000 g mol^{-1}, PEIPA = 1800 g mol^{-1}) was synthesized as described elsewhere.[23c]

The copolymers, which are based on PEG-*b*-PEI with various functional acidic groups −COOH, $-PO_3H_2$, $-SO_3H$, and −SH, were synthesized by further functionalization of the PEI block.[23c] The ethyl phosphonic acid groups were added to the PEI block by Michael-type addition of the amine group to the vinyl-activated group of vinylphosphonic acid to give PEG-*b*-PEI-$(CH_2{-}CH_2{-}PO_3H_2)_n$(PEG-*b*-PEI-PEPA).[23c] PEG-*b*-PEI can also be modified by a simple standard acylation reaction of an amine group of PEI with acyl chloride such as lauroyl chloride ($C_{11}H_{23}COCl$) and will generate PEG-*b*-PEI($CH_2{-}CH_2{-}PO_3H_2$)-$COC_{11}H_{23}$ (lauroyl).[23c] PEG-*b*-PEI-$(CH_2{-}CH_2{-}CH_2{-}SO_3H_2)_n$(PEG-*b*-PEIPSA) was obtained by introduction of a propane sulfonic acid group to the PEI part by means of nucleophilic reaction of the amine group with 1,3-propane sultone.[23c] The reaction of the primary amino groups and also some secondary amino groups with methyl isothiocyanate produced PEG-*b*-PEI$(HS{=}C{-}NCH_3)_n$-$COC_{11}H_{23}$.[23c] The partially phosphorylated poly(hydroxyethyl ethylene) block copolymer with PEG (PEG-*b*-PHEE-PO_4H_2(30 %)) was synthesized as described in ref. [29]. A PEG-poly(aminoamine) dendrimer copolymer (PEG-*b*-STARBURST)(PEG, $M_W = 5000$, Starburst, $M_W = 1400$) was also used in this study as described previously.[33] For the crystallization experiments, all copolymers were purified by exhaustive dialysis.

Hashemite crystallization: The precipitation of $BaCrO_4$ in the presence of various additives was carried out in both 5 mL glass and polypropylene bottles. The polymer concentration was kept at 1 g L^{-1}, respectively. In a typical synthesis, $BaCl_2$ (0.12 mL; 0.05 M, Sigma Aldrich, 99 %) was added to 3 mL polymer solution (c = 1 g L^{-1}) under vigorous stirring at room temperature, resulting in a final $BaCrO_4$ concentration of 2 mM. After

  0947-6539/02/0813-2944 $ 20.00+.50/0 *Chem. Eur. J.* **2002**, *8*, No. 13

3 min, 0.12 mL Na_2CrO_4 (0.05 M, Sigma Aldrich, 99 %) solution was added dropwise to the solution. After a further 3 min stirring, the solution was left for two to five days before the precipitates were collected for characterization. The precipitates were left to stand in their mother solutions for at least 24 h to ensure complete equilibration. The influence of temperature on the crystallization was investigated by using a commercial Teflon-lined autoclave of 40 mL capacity as the reactor (SAINPLATEC Company, Japan). In a typical procedure, both glass bottles and polypropylene bottles, which contained 3 mL of a solution prepared as described before, were sealed and put in to the autoclave and the temperature increased to 50–100 °C in a dry box for 12 h. The autoclave was then taken out and allowed to cool naturally in air. The precipitate was collected for further characterization.

In some cases, aliquots of the solution were poured into a series of 1.5 mL polypropylene tubes (Plastibrand), each containing a carbon-coated, Formvar-covered, copper TEM grid (3 mm in diameter) which was carefully put at the bottom of the tubes with the carbon film exposed to the solution. The copper grids were taken out of the solution after various time intervals, allowed to dry in air, and directly used for TEM and SEM observation.

Characterization: To ensure clear observation of the samples, all precipitates were carefully washed repeatedly with distilled water and then stirred gently before placing one drop of the solution onto copper TEM grids and SEM stubs, respectively. In some cases, the solutions containing precipitates were put in a sonic bath for 3 min to ensure good dispersion of the particles in the solution. The characterization was done using scanning electron microscopy (SEM) on a DSM 940 A (Carl Zeiss, Jena) microscope, and by transmission electron microscopy (TEM) with a Zeiss EM 912 Omega microscope. Dry powder samples were used for the measurements of X-ray powder diffraction (XRD) using a PDS 120 (Nonius GmbH, Solingen) with $Cu_{K\alpha}$ radiation. The computer modeling was done with the *Cerius*^{2} software (Accelrys).

Acknowledgements

We acknowledge financial support from the Max Planck Society and the DFG(SFB 448). S.-H. Yu thanks the Alexander von Humboldt Foundation for granting a research fellowship. H.C. thanks the Dr. Hermann Schnell foundation for financial support. Prof. Dr. M. Sedlak and Dr. Jan Rudloff are acknowledged for leaving the polymers at our disposal and Dr. Yitzhak Mastai is thanked for helpful discussions.

[1] a) D. D. Archibald, S. Mann, *Nature* **1993**, *364*, 430–433; b) S. Mann, G. A. Ozin, *Nature* **1996**, *382*, 313–318; c) H. Yang, N. Coombs, G. A. Ozin, *Nature* **1997**, *386*, 692–695; d) M. Li, H. Schnablegger, S. Mann, *Nature* **1999**, *402*, 393–395.

[2] E. Matijević, *Curr. Opin. Colloid Interface Sci.* **1996**, *1*, 176–183.

[3] X. G. Peng, L. Manna, W. D. Yang, J. Wickham, E. Scher, A. Kadavanich, A. P. Alivisatos, *Nature* **2000**, *404*, 59–61; L. Manna, E. C. Scher, A. P. Alivisatos, *J. Am. Chem. Soc.* **2000**, *122*, 12700–12706.

[4] a) T. S. Ahmadi, Z. L. Wang, T. C. Green, A. Henglein, M. A. El-Sayed, *Science* **1996**, *272*, 1924–1926; b) C. P. Gibson, K. Putzer, *Science* **1995**, *267*, 1338–1340; c) M. P. Pileni, B. W. Ninham, T. Gulik-Krzywicki, J. Tanori, I. Lisiecki, A. Filankembo, *Adv. Mater*. **1999**, *11*, 1358–1362; M. P. Pileni, T. Gulik-Krzywicki, J. Tanori, A. Filankembo, J. C. Dedieu, *Langmuir* **1998**, *14*, 7359–7363; d) Y. Zhou, S. H. Yu, C. Y. Wang, X. G. Li, Y. R. Zhu, Z. Y. Chen, *Adv. Mater.* **1999**, *11*, 850–852; e) S.-J. Park, S. Kim, S. Lee, Z. G. Khim, K. Char, T. Hyeon, *J. Am. Chem. Soc.* **2000**, *122*, 8581–8582.

[5] C. M. Lieber, *Solid State Commun.* **1998**, *107*, 607–616.

[6] J. T. Hu, T. W. Odom, and C. M. Lieber, *Acc. Chem. Res.* **1999**, *32*, 435–445; A. M. Morales, C. M. Lieber, *Science* **1998**, *279*, 208–211.

[7] a) J. D. Klein, R. D. Herrick, D. Palmer, M. J. Sailor, C. J. Brumlik, C. R. Martin, *Chem. Mater.* **1993**, *5*, 902–904; b) C. R. Martin, *Science* **1996**, *266*, 1961–1966; c) D. Routkevitch, T. Bigioni, M. Moskovits, J. M. Xu, *J. Phys. Chem.* **1996**, *100*, 14037–14047.

[8] X. F. Duan, C. M. Lieber, *Adv. Mater.* **2000**, *12*, 298–302; X. F. Duan, C. M. Lieber, *J. Am. Chem. Soc.* **2000**, *122*, 188–189; M. S. Gudiksen, C. M. Lieber, *J. Am. Chem. Soc.* **2000**, *122*, 8801–8802.

[9] a) A. Stein, S. W. Keller, T. E. Mallouk, *Science* **1993**, *259*, 1558–1564; b) T. J. Trentler, K. M. Hickman, S. C. Goel, A. M. Viano, P. C. Gibbons, W. E. Buhro, *Science* **1995**, *270*, 1791–1794; c) S. H. Yu, M. Yoshimura, *Adv. Mater.* **2002**, *14*, 296–300.

[10] See review and references therein: L. A. Estroff, A. D. Hamilton, *Chem. Mater.* **2001**, *13*, 3227–3235.

[11] S. E. Friberg, J. F. Wang, *J. Dispersion Sci. Technol.* **1991**, *12*, 387–402.

[12] S. Mann, D. D. Archibald, J. M. Didymus, T. Douglas, B. R. Heywood, F. C. Meldrum, N. J. Reeves, *Science* **1993**, *261*, 1286–1292; D. Walsh, J. D. Hopwood, S. Mann, *Science* **1994**, *264*, 1576–1578.

[13] J. D. Hopwood, S. Mann, *Chem. Mater.* **1997**, *9*, 1819–1828.

[14] G. D. Rees, R. Evans-Gowing, S. J. Hammond, B. H. Robinson, *Langmuir* **1999**, *15*, 1993–2002.

[15] L. M. Qi, J. Ma, H. Cheng, Z. Zhao, *J. Phys. Chem. B* **1997**, *101*, 3460–3463.

[16] J. Economy, D. T. Meloon, R. L. Ostrozynski, *J. Catalysis* **1965**, *4*, 446–453.

[17] T. Adamski, *Nature* **1961**, *190*, 524.

[18] L. A. Bromley, D. Cottier, R. J. Davey, B. Dobbs, S. Smith, B. R. Heywood, *Langmuir* **1993**, *9*, 3594–3599.

[19] W. J. Benton, I. R. Collins, I. M. Grimsey, G. M. Parkinson, S. A. Rodger, *Faraday Discuss.* **1993**, *95*, 281–297.

[20] P. V. Coveney, R. Davey, J. L. W. Griffin, Y. He, J. D. Hamlin, S. Stackhouse, A. Whiting, *J. Am. Chem. Soc.* **2000**, *122*, 11557–11558.

[21] R. J. Davey, S. N. Black, L. A. Bromley, D. Cottier, B. Dobbs, J. E. Rout, *Nature* **1991**, *353*, 549–550.

[22] A. L. Rohl, D. H. Gay, R. J. Davey, C. R. A. Catlow, *J. Am. Chem. Soc.* **1996**, *118*, 642–648.

[23] a) See recent review and references therein:H. Cölfen, *Macromol. Rapid. Commun.* **2001**, *22*, 219–252; b) M. Sedlak, M. Antonietti, H. Cölfen, *Macromol. Chem. Phys.* **1998**, *199*, 247–254; c) M. Sedlak, H. Cölfen, *Macromol. Chem. Phys.* **2001**, *202*, 587–597.

[24] a) H. Cölfen, M. Antonietti, *Langmuir* **1998**, *14*, 582–589; b) H. Cölfen and L. M. Qi, *Chem. Eur. J.* **2001**, *7*, 106–116; c) J. M. Marentette, J. Norwig, E. Stockelmann, W. H. Meyer, G. Wegner, *Adv. Mater.* **1997**, *9*, 647–651.

[25] M. Antonietti, M. Breulmann, C. Göltner, H. Cölfen, K. K. Wong, D. Walsh, S. Mann, *Chem. Eur. J.* **1998**, *4*, 2493–2500.

[26] a) L. M. Qi, H. Cölfen, M. Antonietti, *Angew. Chem. Int. Ed.* **2000**, *39*, 604–607; b) L. M. Qi, H. Cölfen, M. Antonietti, *Chem. Mater.* **2000**, *12*, 2392–2403; c) L. M. Qi, H. Cölfen, M. Antonietti, M. Lei, J. D. Hopwood, A. J. Ashley, S. Mann, *Chem. Eur. J.* **2001**, *7*, 3526–3532.

[27] M. Öner, J. Norwig, W. H. Meyer, G. Wegner, *Chem. Mater.* **1998**, *10*, 460–463.

[28] a) P. Hartman, W. G. Perdock, *Acta Crystallogr.* **1955**, *8*, 524–529; b) P. Hartman, S. S. Strom, *J. Cryst. Growth.* **1989**, *97*, 502–512; c) A. Fernández-González, R. Martín-Díaz, and M. Prieto, *J. Cryst. Growth* **1999**, *200*, 227–235.

[29] J. Rudloff, M. Antonietti, H. Cölfen, J. Pretula, K. Kaluzynski, S. Penczek, *Macromol. Chem. Phys.* **2002**, in press; J. Rudloff, PhD thesis, Potsdam, **2001**.

[30] a) R. Kniep, S. Busch, *Angew. Chem. Intl. Ed.* **1996**, *35*, 2624–2626; b) S. Busch, H. Dolhaine, A. DuChesne, S. Heinz, O. Hochrein, F. Laeri, O. Podebrad, U. Vietze, T. Weiland, R. Kniep, *Eur. J. Inorg. Chem.* **1999**, *10*, 1643–1653; c) S. Busch, PhD thesis, Darmstadt 1998; d) H. Cölfen, Habilitation thesis, Potsdam, **2001**; e) H. Cölfen, L. M. Qi, *Progr. Colloid Polym. Sci.* **2001**, *117*, 200–203.

[31] J. Rieger, E. Hädicke, I. U. Rau, D. Boeckh, *Tenside Surfactants Deterg.* **1997**, *34*, 430–435.

[32] G. R. Kieczykowski, R. B. Jobson, D. G. Melillo, D. F. Reinhold, V. J. Grenda, I. Shinkai, *J. Org. Chem.* **1995**, *60*, 8310–8312.

[33] L. M. Qi, H. Cölfen, M. Antonietti, *Nano. Lett.* **2001**, *1*, 61–65.

Received: December 27, 2001
Revised: February 27, 2002 [F3760]